RESEARCH ARTICLE

Editorial Process: Submission:05/31/2025 Acceptance:11/15/2025 Published:11/22/2025

Dual Repurposing Strategy: Rivaroxaban and Ciprofloxacin as a Synergistic Anticancer Therapy in Cervical Cancer: Insight into Inhibition of Metastasis via Targeting the EMT Pathway

Alyaa Aziz Ahmed*

Abstract

Objective: This study assessed the anticancer and antimetastatic impact of rivaroxaban-ciprofloxacin mixture and explored its molecular mechanism by examining its ability to target the epithelial-mesenchymal transition (EMT) pathway. Methods: Following incubation periods of 24 and 72 hours, HeLa and normal human fibroblast (NHF) cell lines were employed to investigate the anticancer and safety properties of rivaroxaban, ciprofloxacin, rivaroxabanciprofloxacin mixture, and carboplatin, with concentrations varying from 0.1 to 1000 μg/ml. The wound healing assay (WHA) of cervical cancer cells was employed to assess the anti-metastatic effects of the mixture at three time points: 0, 12, and 24 hours.. A combination index (CI) and selectivity toxicity index (SI) score were estimated to assess the potential synergistic effects of the mixture's components and their selectivity toxicity. A computational molecular docking simulation was conducted to evaluate the binding affinity of rivaroxaban and ciprofloxacin to different regulatory signals in the EMT pathway. Results: The MTT and WHS assays outcomes revealed that the rivaroxaban-ciprofloxacin mixture possesses anticancer and antimetastatic properties. This combination significantly suppresses the growth of cervical cancer cells more effectively than carboplatin, rivaroxaban, or ciprofloxacin alone. Additionally, the mixture results in a 98% delay of cancer cell migration after 24 hours of incubation. Furthermore, the mixture's cytotoxicity on NHF cells was significantly lower than carboplatin. The combination of rivaroxaban and ciprofloxacin showed synergistic cytotoxic effects, as confirmed by the CI score. Also, it displays a selective cytotoxicity toward cancer cells, as indicated by the SI score. The molecular docking study results revealed that the most favorable interactions for rivaroxaban and ciprofloxacin occurred with the matrix metalloprotease and Tankyrase enzyme, with docking scores of -9 kcal/mol and -8.9 kcal/mol, respectively. Conclusion: The study's findings and the established pharmacokinetic and safety profiles of mixture drugs suggest that the pairing of rivaroxaban and ciprofloxacin offers a promising and safer option for treating cervical cancer.

Keywords: Rivaroxaban and ciprofloxacin- matrix metalloprotease- molecular docking- wound healing assay

Asian Pac J Cancer Prev, 26 (11), 4195-4207

Introduction

Cervical cancer poses a major global health challenge, especially in low- and middle-income countries (LMICs), where it is the fourth most prevalent cancer among women [1]. Infections with high-risk types of human papillomavirus (HPV), especially HPV-16 and HPV-18, are the leading cause of around 70% of cases [2, 3]. Even with effective screening programs and HPV vaccination available, disparities in access to these preventive measures result in higher incidence and mortality rates in low- and middle-income countries than in high-income countries [3-5]. Early use of Pap smears and HPV testing has notably reduced cervical cancer rates in areas with strong healthcare systems. Nevertheless, attaining global fairness in prevention and treatment remains a significant

public health challenge [3, 6-9]. Chemoradiotherapy serves as the primary treatment choice for cervical cancer. The chemotherapy used, usually based on cisplatin regimens, encounters substantial challenges such as systemic toxicity, drug resistance, and adverse effects on healthy tissues [10, 11]. The side effects, including nephrotoxicity, myelosuppression, and gastrointestinal distress, frequently reduce patients' quality of life and restrict treatment options [12].

The adverse effects associated with chemotherapy highlight the urgent need for safer alternatives. Numerous trials have been carried out to find a suitable treatment for cervical cancer by repurposing a drug initially developed for different therapeutic applications in cancer [13-21]. In line with this concept, rivaroxaban and ciprofloxacin are examples of medications that may have anticancer effects.

Department of Obstetrics and Gynecology, College of Medicine, Diyala University, Iraq. *For Correspondence: alyaa1977alrubaye@gmail.com

The criteria for selecting these drugs were determined through extensive pharmacokinetic research and safety evaluations. Furthermore, they have shown anticancer effectiveness, supported by numerous earlier studies.

Rivaroxaban, an oral anticoagulant and direct factor Xa inhibitor, has garnered attention for its potential anticancer effects alongside its primary use in thromboembolic disorders. Preclinical research suggests that rivaroxaban may hinder cancer progression by impacting mechanisms like tumor-associated thrombosis, which is connected to tumor growth and metastasis [22]. Moreover, Rivaroxaban has reduced the expression of pro-inflammatory and proangiogenic factors like tissue factor (TF) and vascular endothelial growth factor (VEGF). This action helps to limit tumor angiogenesis and metastasis [23]. Recent findings indicate that rivaroxaban could directly affect cancer cell survival by promoting apoptosis and hindering proliferation via the modulation of signaling pathways like PI3K/AKT [24, 25]. Rivaroxaban is structurally identified by the molecular formula C19H18ClN3O5S. It includes a morpholinone core, a chlorothiophene group, and an oxazolidinone ring, which selectively inhibit Factor Xa. These structural elements improve binding affinity and pharmacokinetics, permitting administration once daily [26]

Additionally, numerous studies have been conducted regarding the possible anticancer effects of another ingredient, ciprofloxacin. A recent survey investigating the repurposing of this fluoroquinolone antibiotic has uncovered its potential as an anticancer agent, emphasizing its ability to affect cellular pathways vital for tumor development. Initially intended for treating bacterial infections, the drug's interaction with DNA gyrase and topoisomerase IV in prokaryotes has piqued interest regarding its influence on eukaryotic topoisomerases, which are frequently overexpressed in cancer cells to facilitate rapid growth. In vitro studies have shown that ciprofloxacin can initiate apoptosis and induce cell cycle arrest across various cancer cell lines. A recent survey of colorectal cancer cells (HCT-116) demonstrated that ciprofloxacin (at concentrations ranging from 50 to 100 μM) activates caspase-3 and decreases cyclin D1 levels, resulting in G1 phase arrest and apoptosis [27-30]. In nonsmall cell lung cancer (A549 cells), ciprofloxacin reduced metastasis by inhibiting epithelial-mesenchymal transition (EMT) via modulation of the TGF-β/Smad3 pathway [31-33]. Animal models bolster these conclusions. A 2023 study on xenograft mice with triple-negative breast cancer (utilizing MDA-MB-231 cells) found that a daily treatment of ciprofloxacin (20 mg/kg) reduced tumor growth by 40% by inducing ROS-related DNA damage and activating p53 upregulation [34].

Ciprofloxacin's molecular formula is C₁₇H₁₈FN₃O₃. Its structure features a fluorine atom at position six and a piperazine ring at position 7, contributing to enhanced DNA gyrase inhibition and improved bacterial cell penetration. The bicyclic quinolone core provides broadspectrum activity, making it effective against Gramnegative and some Gram-positive pathogens [35].

Understanding the EMT pathway is crucial for developing effective cancer therapies, as it is closely linked

to cancer metastasis. The current study highlights how the combination addresses this significant pathway in cancer.

Matrix metalloproteases and Tankyrase enzymes are vital regulatory factors in the EMT pathway. These zinc-dependent enzymes drive cancer progression by degrading ECM proteins, promoting invasion, metastasis, and angiogenesis. MMP-2 and MMP-9 are key aggressiveness markers due to their collagen-cleaving ability. They also modulate tumor signaling by releasing growth factors. However, some MMPs, like MMP-8, can suppress tumors, highlighting their context-dependent roles in cancer biology [36-38]. MMP-2 and MMP-9 drive cervical cancer progression by degrading ECM, promoting invasion, metastasis, and angiogenesis, making them potential therapeutic targets [39]. Several studies have investigated matrix metalloproteinase (MMP)targeted therapies, emphasizing the use of agents such as Batimastat and Tanomastatin. These selective inhibitors operate by mitigating the pro-tumorigenic effects of MMPs while maintaining normal physiological functions [40]. However, clinical success is still restricted due to the complicated relationships of MMPs within the tumor [41].

Additionally, Tankyrase (TNKS), an enzyme belonging to the PARP family, promotes cancer progression by stabilizing AXIN2 and activating Wnt/β-catenin signaling. It enhances proliferation, stemness, and chemoresistance in colorectal, breast, and ovarian cancers. Its increased expression is linked to metastasis and unfavorable outcomes. Recent research also indicates that TNKS modifies the tumor microenvironment, affecting immune evasion and angiogenesis, posing it as a potential therapeutic target [42]. Another study showed that Tankyrase inhibitors XAV939 and G007-LK impede Wntdriven tumor growth in preclinical testing [43].

Despite the numerous studies on this issue, they have been insufficient in demonstrating the anticancer and antimetastatic effects of the rivaroxaban-ciprofloxacin combination and its ability to target regulatory enzymes in the EMT pathway. To address this gap, the present study assessed the anticancer properties of the rivaroxaban-ciprofloxacin mixture, examining its antimetastatic impact and underlying molecular mechanisms by evaluating its ability to target the EMT pathway.

Materials and Methods

Study medication

Study medications were sourced as raw materials from the Samarra Pharmaceutical Factory in Iraq. Both drugs and their mixture underwent serial dilution using MEM media, resulting in concentrations ranging from 0.1 to 1000 μ g/ml. For the rivaroxaban-ciprofloxacin mixture, the concentrations were adjusted from 0.05 to 50 μ g/ml for each drug, culminating in a final concentration of 0.1 to 1000 μ g/ml.

Cytotoxicity study

A cytotoxicity assessment was conducted on the human cervical cancer cell line (HeLa) to investigate the anticancer properties of rivaroxaban, ciprofloxacin, Carboplatin, and the mixture. Additionally, the cytotoxic effects of this mixture on the NHF cell line, which serves as a "normal healthy cell line," were analyzed to evaluate its safety and determine if any drug interactions could negatively impact normal cells.

The cytotoxic and safety profiles of rivaroxaban, ciprofloxacin, Carboplatin, and the mixture were assessed by measuring the viability of cancerous and normal healthy cells at 0.1 to $100 \mu g/ml$ concentrations.

Cell Lines

Cancer and normal healthy cell lines were employed, including the HeLa cell line, which originates from human cervical cancer tissue [27, 44]. And the NHF cell line, which originates from Normal human-derived adipose tissue [45].

Tissue culture conditions

MEM media (US Biological, USA) was used to grow cell lines, supplemented with 10% (v/v) fetal bovine serum (FBS) (Capricorn-Scientific, Germany), 100 IU of penicillin, and 100 μg of streptomycin to avoid bacterial contamination. The cells were incubated in a humidified atmosphere at 37 °c using exponentially growing cells [46].

cytotoxicity study

MTT assay is a colorimetric assay that utilizes the capacity of live cells to convert MTT stain into purple formazan crystals, which is made possible by the dehydrogenase enzyme produced by mitochondria. In the MTT assay, cells are typically cultured in a 96-well plate and exposed to different concentrations of test agents. After an incubation period, MTT is added to each well and incubated again. Viable cells convert MTT into formazan, which can be solubilized, and its concentration is quantified by measuring the absorbance at a specified wavelength using a spectrophotometer.

The quantity of viable cells influences the level of formazan production. A reduction in formazan production after applying the tested medications indicates cytotoxicity, which impacts absorbance. The doseresponse curve helps identify the half-maximal inhibitory concentration (IC50), which refers to the concentration of the tested medications that decreases cell viability by 50%. It's calculated via employed GraphPad Prism (version 9.5.0 (750) [19, 47].

Cells were placed in a 96-well microplate at a density of 10,000 cells per well and incubated at 37 °C for 24 hours until they became confluent. The MTT cytotoxicity assay utilized six wells for each concentration of rivaroxaban, ciprofloxacin, Carboplatin, and the mixture. Cells were treated with concentrations (0.1, 1, 10, 100, and 1000 $\mu g/ml$). A negative control was set up with several untreated wells. Following 24 and 72 hours of treatment, 28 μL of MTT dye solution (2 mg/ml) was introduced to each well, followed by three hours of incubation. Afterward, 100 μL of DMSO was added to each well and incubated for 15 minutes. Optical density readings were taken at 570 nm using a microplate reader. The following equation is employed to calculate the percentage of growth inhibition [48].

$$\textit{Growth inhibition} \% = \frac{\textit{optical density of control wells} - \textit{optical density of treated wells}}{\textit{optical density of control wells}} * 100\%$$

Selective toxicity index

The selective toxicity index score was estimated to scrutinize the selective toxicity of the rivaroxaban-ciprofloxacin mixture and carboplatin against cancer cells over 24 and 72 hours of incubation. Once the IC50 levels for the mixture and carboplatin were established, the selective cytotoxicity index was determined using a mathematical formula based on cellular growth curves for both HeLa and NHF cell lines [49].

Selective toxicity Index (SI) =
$$\frac{IC 50 \text{ of normal cell lines}}{IC 50 \text{ of cancer cell lines}}$$

An SI score above 1.0 indicates a drug's enhanced targeting of tumor cells compared to its toxicity towards normal cells.

Wound-healing Assay

A wound-healing assay was employed to identify the ability of the mixture to inhibit cancer cell metastasis. HeLa cells were seeded in a 6-well plate at $1.5\times10^{\circ}6$ cells/well in 1.0 mL of media with serum. The cells were then incubated for 24-48 hours to achieve confluency. A marker pen was used to draw horizontal lines evenly on the back of the 6-well plate, spaced 0.5-1 cm apart, crossing through the holes. Once the cells reached 90-100% confluency, a gentle, straight scratch was made using a sterile $200~\mu$ L pipette tip. Next, the cells were washed three times with PBS to remove the scratched cells, followed by adding a Low serum medium (5% FBS), and cultured at 37~°C in a 5% CO2 atmosphere incubator.

Untreated (control wells) and treated wells with each of the following (rivaroxaban, ciprofloxacin, and mixture) were incubated for 0, 12, and 24 hours. Cell migration at the scratch site was observed under an inverted microscope at the time of scratching and at the end of the incubation period. The distances of the wound area were estimated after capturing images using Image J software. After calculating the wound area at 0, 12, and 24 hours of incubation, the percentage of wound closure can be calculated by applying the following equation [50].

% wound closure =
$$\left(1 - \frac{At}{A^{\circ}}\right) * 100$$

(At: the wound area at a specific time. A°: Wound area at zero time)

Molecular docking

Using the ChemDraw application (Cambridge Soft, USA), the chemical structures of rivaroxaban and ciprofloxacin were generated and refined with Chem3D version. Based on the outcomes of a pilot study to explore the chemical docking of rivaroxaban and ciprofloxacin with the regulatory signals of epithelial-mesenchymal transition EMT pathway, Tankyrase and matrix metalloproteinase enzymes were selected. The molecular structures of each enzyme were obtained from

the Protein Data Bank, with the codes (PDB:4w5s) and (PDB:2oxu) for each enzyme, respectively.

Enzyme structures were optimized and adjusted utilizing AutoDock Tools. This software identified the best configuration for the ligands and produced a PDBQT file for them. After optimization, the structures of the ligands, rivaroxaban and ciprofloxacin, as well as the human Tankyrase and matrix metalloproteinase enzymes, were entered into AutoDock Tools. The docking procedure was subsequently carried out using the same application. The docking energy scores and binding interactions were assessed through BIOVIA Discovery Studio, UCSF Chimera, and AutoDock Vina [51, 52].

Drug Interaction Mapping (Combination Index- CI) Scoring

Compusyn, a computational simulator, calculated the combination index (CI) scores. This evaluation aimed to assess the potential for synergistic, additive, or antagonistic interactions among the mixture components. Concentration-effect curves illustrate the percentage of cells that show reduced growth relative to drug concentration, assessed after 24 and 72 hours of treatment.

CI values below 1 indicate synergistic effects, values equal to 1 suggest additivity, and values above 1 represent antagonism. The combination index was calculated using Compusyn software (Biosoft, Ferguson, MO, USA) values [53, 54].

(dose reduction index- DRI) Scoring

Compusyn, a computational simulator, was utilized to calculate dose reduction index (DRI) scores. The DRI score estimates how much the concentration of each drug in a mixture can be lowered while still preserving its cytotoxic effectiveness.

A DRI score greater than 1 signifies an advantageous reduction in concentration, whereas a score below 1 suggests a disadvantageous reduction. The Compusyn software (Biosoft, Ferguson, MO, USA) performed the DRI calculations [53, 54].

Ethical approval

This research exclusively utilized in vitro cell line models, with no experiments involving human participants or laboratory animals. All research methods complied with institutional ethical standards for laboratory investigations.

Statistical Analysis

The cytotoxicity assay results are presented as mean \pm standard deviation (SD). A one-way analysis of variance (ANOVA) was conducted to assess variation among the research groups. Differences between individual groups were analyzed using the paired t-test and LSD tests. Statistical analysis was performed using SPSS version 20, with a significance level of p < 0.05 [55].

The study used lowercase and uppercase letters in data tables to differentiate between statistical groupings or significance levels. Means (averages) that share the same letter are not significantly different, whereas means assigned different letters are statistically significant. This

approach offers a fast and straightforward way to convey intricate statistical results without elaborate explanations. Readers can quickly understand which groups are alike or distinct based on the letters assigned.

Results

Cytotoxic study

We first evaluated the cytotoxicity of rivaroxaban and ciprofloxacin separately, then assessed their combined effects. This preliminary evaluation aimed to clarify the mechanisms of cytotoxicity and analyze the interactions between the mixture's components, specifically determining whether these interactions exhibit synergistic, antagonistic, or additive effects.

Rivaroxaban Cytotoxicity

Rivaroxaban showed the ability to inhibit cervical cancer growth; cytotoxicity significantly rises with increased rivaroxaban concentrations and extended incubation durations. The influence of incubation time on cytotoxicity was more pronounced than that of concentration (Table 1).

Ciprofloxacin cytotoxicity

In the same line as rivaroxaban cytotoxicity, ciprofloxacin also showed an ability to inhibit the growth of cervical cancer, with a pattern that depended on the ciprofloxacin concentration and time of incubation (Table 2).

Carboplatin cytotoxicity

Carboplatin was chosen as a positive control for comparative purposes. To determine its selective toxicity, its cytotoxicity against each cancer cell and a healthy normal cell was tested.

The cytotoxicity assay of carboplatin indicated that its cytotoxic effects on each cell line depended on the concentration and duration of exposure (Table 3).

(Rivaroxaban -ciprofloxacin) mixture cytotoxicity

The study findings showed that combining rivaroxaban and ciprofloxacin suppressed cervical cancer growth, with the extent of inhibition mainly affected by the mixture's concentration and the incubation duration. Additionally, the mixture's cytotoxic effect on the NHF cell line was significantly less than its effect on the cancer cell line, indicating a favorable safety profile and targeted toxicity towards cancer cells (Tables 4,5).

The comparison of cytotoxicity among the mixture, rivaroxaban, ciprofloxacin, and carboplatin showed that the mixture has significantly higher cytotoxicity than any of these drugs alone, especially at higher concentration levels for each incubation period, indicating a synergistic cytotoxic effect among the components of the mixture and positioning it as a superior alternative to traditional chemotherapy treatments Supplementary Tables (1,2).

Selective toxicity index assessment

The selectivity index (SI) for the rivaroxaban-ciprofloxacin mixture was 2.33 and 14.99 at 24 and 72

Table 1. The Effect of Rivaroxaban on the Survival Rates of Cervical Cancer Cells at 24 and 72 Hours

Concentration (µg/ml)	Cellular proliferation inhi	P- value	
	24 hr.	72 hr.	
0.1	$C \ 3.00 \pm 1.000$	$C\ 14.00 \pm 4.000$	0.010*
1	BC 12.00 ± 2.000	$B\ 27.00 \pm 2.000$	0.001*
10	$AB\ 23.00 \pm 3.000$	$B\ 34.00 \pm 3.000$	0.005*
100	$A\ 34.00 \pm 4.000$	$A\ 47.00 \pm 3.000$	0.011*
1000	$A 33.00 \pm 4.000$	$A\ 45.00 \pm 1.000$	0.007*
LSD value	11.04	10.16	
IC ₅₀	>1000 µg/ml	$>1000~\mu g/ml$	

^{*,} significant at (P<0.05)

Table 2. The Effect of Ciprofloxacin on the Survival Rates of Cervical Cancer Cells after 24 and 72 Hours

Concentration (µg/ml)	Cellular proliferation inhi	Cellular proliferation inhibition (mean ± SD)		
	24 hr.	72 hr.		
0.1	$C~0.00 \pm 0.000$	$C \ 3.00 \pm 3.000$	0.158*	
1	$C 1.00 \pm 1.000$	$B\ 12.00 \pm 2.000$	0.001*	
10	$C 5.00 \pm 2.000$	$B\ 29.00 \pm 2.000$	0.0001*	
100	$B\ 21.00 \pm 1.000$	$A~41.00\pm1.000$	0.0001*	
1000	$A\ 30.00 \pm 3.000$	$A~46.00\pm1.000$	0.001*	
LSD value	6.3	7.1		
IC 50	>1000 µg/ml	>1000 µg/ml		

^{*,} significant at (P<0.05)

hours, respectively, demonstrating that this mixture was more selective in targeting cancer cells than its effects on healthy cells. Additionally, the SI increased with more extended incubation periods. The SI for carboplatin was 0.856 and 0.243 at 24 and 72 hours, reflecting a lower selectivity for cancer cells than its effects on healthy cells (Figure 1).

Wound-healing Assay

During wound healing, cervical cancer cells proliferate and migrate to close the wound and restore the confluent monolayer [56]. Multiple wells containing HeLa cells, treated with rivaroxaban, ciprofloxacin, and their mixture, were scratched and incubated for 12 and 24 hours to evaluate the ability of the combination of rivaroxaban and ciprofloxacin to delay migration rates. The effect of time on the migration rate for each treatment was assessed.

ImageJ was used to estimate the cell-free area, and the cell migration rate was calculated by determining the reduction in the cell-free area as a percentage of the wound closure.

This finding indicates that after 12 hours of incubation, the wound closure percentage was 44% for untreated wells, compared to 10%, 43%, and 9% for rivaroxaban, ciprofloxacin, and the mixture, respectively. After 24 hours of incubation, the percentage of wound closure increased to 98% for untreated wells, while it was 32%, 76%, and 9% for rivaroxaban, ciprofloxacin, and the mixture, respectively.

Statistically, the findings indicated that the wound closure caused by rivaroxaban and the mixture after 12 hours of incubation was lower than that caused by ciprofloxacin. After 24 hours of incubation, the mixture displays a significant delay in wound closure compared to the other treatments. Supplementary Table

Table 3. The Effect of Carboplatin on the Viability of HeLa and NHF Cell Lines after 24 and 72 Hours

Concentration (µg/ml)	Cellular proliferation inhibition (mean \pm SD)					
	HeLa cell line			NHF cell line		
	24 hr.	72 hr.	P- value	24 hr.	72 hr.	P- value
0.1	$D\ 1.00\pm1.000$	$D\ 6.00 \pm 2.000$	0.018*	$D\ 3.00 \pm 2.000$	$D 9.00 \pm 2.000$	0.021*
1	$CD\ 7.00\pm2.000$	$CD\ 13.00 \pm 3.000$	0.045*	$CD\ 12.00 \pm 2.000$	$D\ 20.00 \pm 5.000$	0.062
10	$C\ 12.00 \pm 2.000$	$C\ 21.00 \pm 1.000$	0.002*	$C\ 20.00 \pm 2.000$	$C\ 33.00 \pm 3.000$	0.003*
100	$B\ 30.00 \pm 3.000$	$B\ 44.00 \pm 4.000$	0.008*	$B\ 36.00 \pm 2.000$	$B\ 47.00 \pm 3.000$	0.006*
1000	$A\ 42.00 \pm 2.000$	$A\ 54.00\pm2.000$	0.002*	$A\ 54.00 \pm 4.000$	$A\ 68.00 \pm 2.000$	0.006*
LSD value	7.64	9.48	-	9.2	11.62	-
IC ₅₀	$>1000~\mu g/ml$	$601.4~\mu g/ml$	-	856.4 μg/ml	$146.2~\mu g/ml$	-

^{*,} significant at (P<0.05)

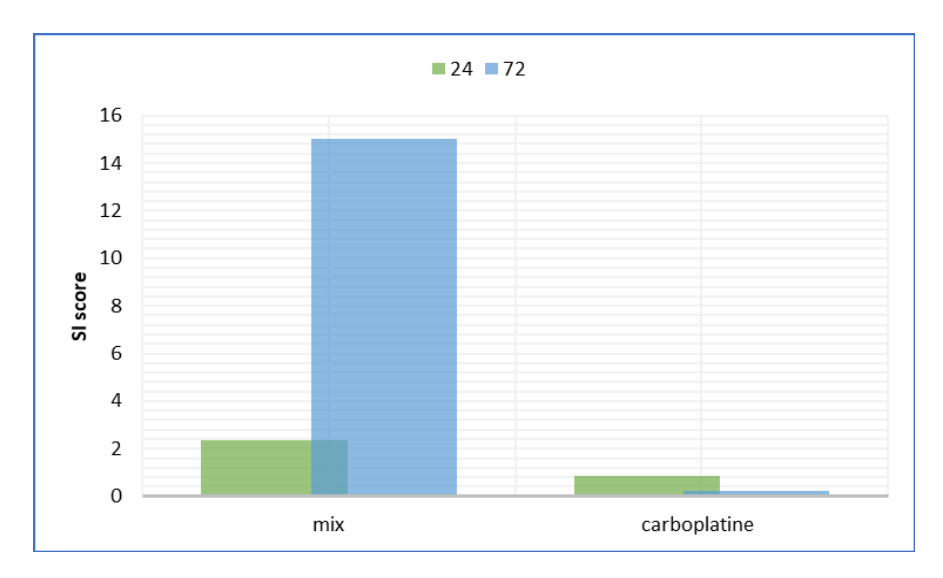


Figure 1. Comparison of the Mixture with Carboplatin SI at 24 and 72 Hours. (An SI above 1.0 suggests a drug is more effective against tumor cells than normal cells.)

Table 4. The Impact of Mixture on the Survival Rates of HeLa and NHF Cell Lines at 24 and 72 Hours

Concentration	Cellular proliferation inhibition (mean \pm SD)						
(µg/ml)	HeLa cell line			NHF cell line			
	24 hr.	72 hr.	P- value	24 hr.	72 hr.	P- value	
0.1	$D\ 11.00 \pm 1.000$	$D\ 31.00 \pm 4.000$	0.001*	$C~0.00\pm0.000$	$D\ 0.00 \pm 0.000$	N. S	
1	$C\ 24.00 \pm 2.000$	$C\ 40.00 \pm 1.000$	0.0001*	$C~0.00\pm0.000$	$CD\ 3.00\pm2.000$	0.060	
10	$C\ 31.00 \pm 1.000$	$BC\ 46.00 \pm 2.000$	0.0001*	$BC\ 5.00\pm1.000$	$BC\ 10.00 \pm 2.000$	0.018*	
100	$B\ 44.00 \pm 4.000$	$B\ 52.00 \pm 2.000$	0.036*	$AB~8.00\pm3.000$	$AB\ 14.00 \pm 4.000$	0.106	
1000	$A~58.00\pm3.000$	$A\ 71.00 \pm 1.000$	0.002*	$A\ 14.00 \pm 2.000$	$A\ 22.00 \pm 2.000$	0.008*	
LSD value	9.06	8.3	-	6.08	8.62	-	
IC 50	428.5 μg/ml	66.7 µg/ml	-	>1000 µg/ml	>1000 µg/ml	-	

3 and Figures 2, 3).

Molecular docking studies

A computational molecular docking simulation assessed how the mixture components (rivaroxaban and

ciprofloxacin) interact with the regulatory signals of epithelial-mesenchymal transition (EMT). The findings revealed that rivaroxaban displayed the strongest interaction with the matrix metalloproteinase enzyme (PDB code: 20xu), achieving a docking score of -9 kcal/

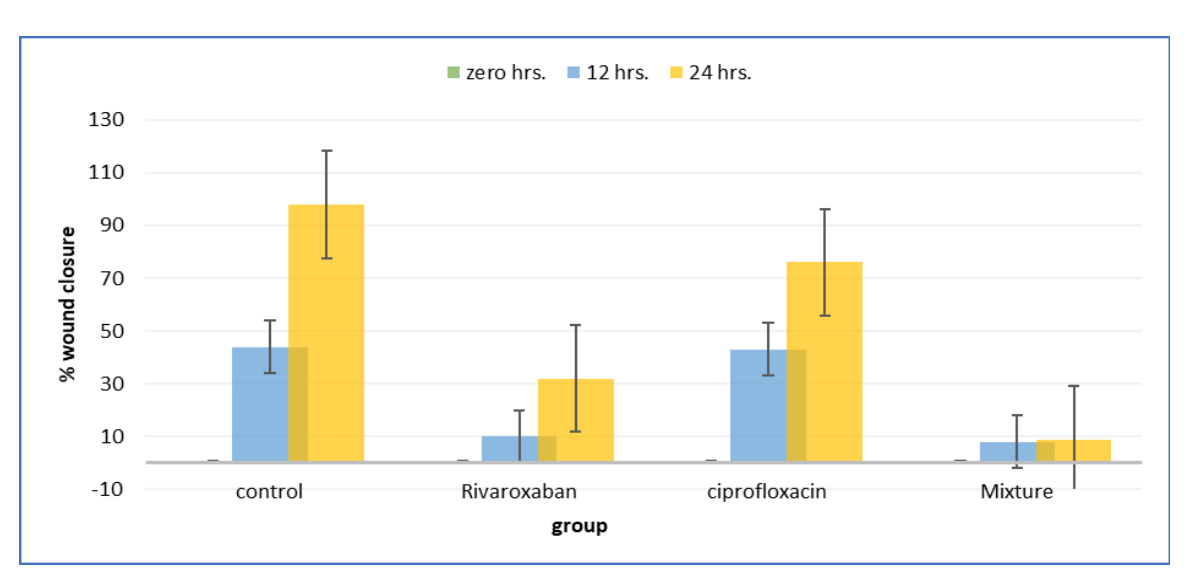


Figure 2. Compares Wound Closure Rates between Untreated and Treated Wells Using Rivaroxaban, Ciprofloxacin, and Their Mixture at 0, 12, and 72 Hours.

4200 Asian Pacific Journal of Cancer Prevention, Vol 26

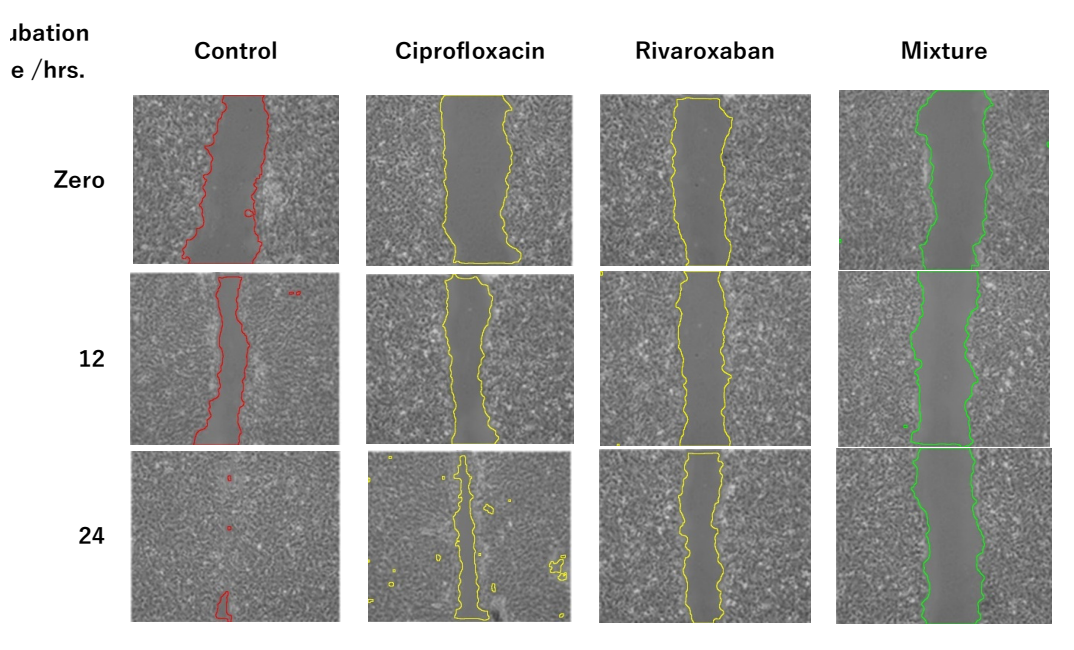


Figure 3. Images from Light Microscopes Depicting Wound Healing assays on HeLa Cancer Cells Treated with Rivaroxaban, Ciprofloxacin, and Their Mixture at 12- and 24-hour post-scratch. 10×.

Table 5. Comparing the Mixture's Effects on the Growth of HeLa and NHF Cell Lines at 24 and 72 Hours

Concentration	Cellular proliferation inhibition (mean \pm SD)						
$(\mu g/ml)$	24 hr.		72 hr.				
	HeLa cell line	NHF cell line	P- value	HeLa cell line	NHF cell line	P- value	
0.1	$D\ 11.00 \pm 1.000$	$C\ 0.00 \pm 0.000$	0.0001*	$D\ 31.00 \pm 4.000$	$D~0.00 \pm 0.000$	0.0001*	
1	$C\ 24.00 \pm 2.000$	$C~0.00\pm0.000$	0.0001*	$C\ 40.00 \pm 1.000$	$CD\ 3.00\pm2.000$	0.0001*	
10	$C\ 31.00 \pm 1.000$	$BC\ 5.00\pm1.000$	0.0001*	$BC\ 46.00 \pm 2.000$	$BC\ 10.00 \pm 2.000$	0.0001*	
100	$B\ 44.00 \pm 4.000$	$AB\ 8.00\pm3.000$	0.0001*	$B\ 52.00 \pm 2.000$	$AB\ 14.00 \pm 4.000$	0.0001*	
1000	$A~58.00\pm3.000$	$A\ 14.00\pm2.000$	0.0001*	$A\ 71.00 \pm 1.000$	$A\ 22.00 \pm 2.000$	0.0001*	
LSD value	9.06	6.08	-	8.3	8.62	-	
IC 50	428.5 μg/ml	>1000 µg/ml	-	66.7 μg/ml	>1000 µg/ml	-	

^{*,} significant at (P<0.05)

mol. In contrast, ciprofloxacin exhibited a greater affinity for interaction with Tankyrase (PDB code: 4w5s), resulting in a docking score of -8.9 kcal/mol. The study employed AutoDock tools version 1.5.7, BIOVIA Discovery Studio, UCSF Chimera, and AutoDock Vina [57].

Analysis of molecular docking for the interaction

of rivaroxaban with matrix metalloproteinase yields one "conventional hydrogen bond" with the THR A:239 amino acid residue at A distance of 2.90 Å. Two "carbon-hydrogen bonds" occur with ALA A:234 and LYS A:241 amino acid residues at distances of 3.14 Å and 3.22 Å, respectively. One "pi-cation bond" is formed

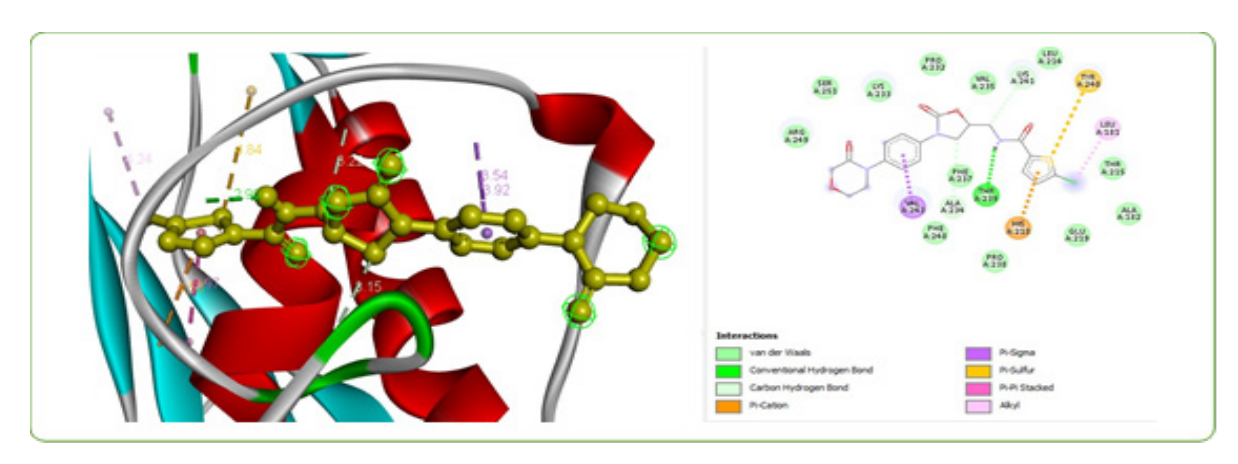


Figure 4. Binding Site Structure in 2D and 3D for Human Matrix Metalloproteinase with Rivaroxaban

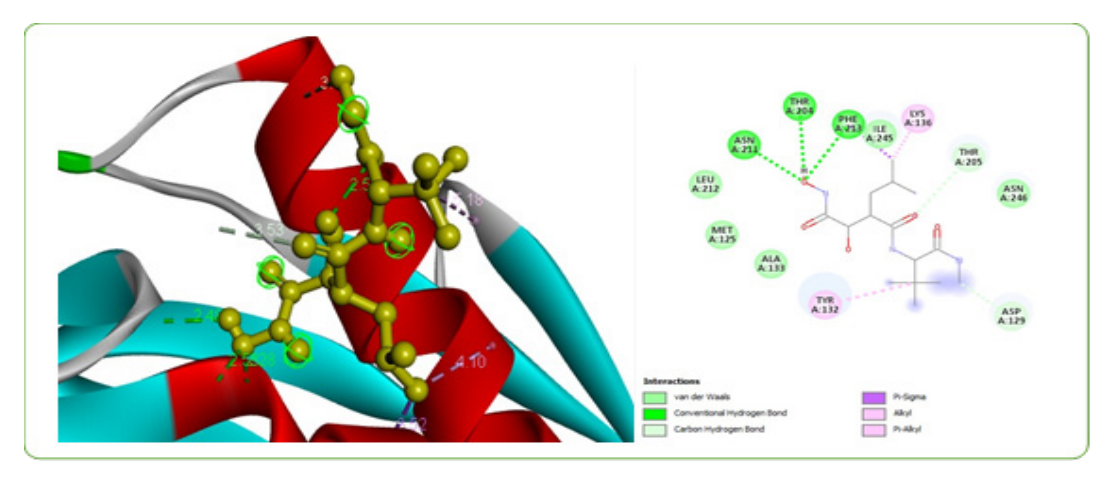


Figure 5. Binding Site Structure in 2D and 3D for Human Matrix Metalloproteinase with Marimastat

with HIS A:218 amino acid residue at a distance of 4.52 Å. Two "pi-sigma bonds" are formed with two VAL A:243 amino acid residues at distances of 3.54 Å and 3.92 Å. Subsequently, one "pi-sulfur bond" occurs with TYR A:240 amino acid residue at a distance of 4.83 Å, and one "pi-pi stacked bond" is formed with HIS A:218 amino acid residue at a distance of 3.96 Å. Finally, one "alkyl bond" forms with LEU A:181 amino acid residue at a distance of 4.24 Å (Figure 4).

For comparative purposes, a molecular docking study assessed the interaction between Marimastat, a "matrix metalloproteinase inhibitor." [58], and the matrix metalloproteinase enzyme, resulting in a docking score of -5.9 kcal/mol for binding and presenting. Three "conventional hydrogen bond" constraints with ASN A:211, PHE A:213, and THR A:204 amino acid residues at distances of 2.52 Å, 2.28 Å, and 2.48 Å, respectively. Two "carbon-hydrogen bonds" constrict with THR A:205 and ASP A:129 amino acid residues at distances of 3.53 Å and 3.67 Å, respectively. One "pi-sigma bond" constricts with PHE A:213 amino acid residues at a distance of 3.51 Å. One "alkyl bond" constricts with LYS A:136 amino acid residues at a distance of 4.09 Å. Finally, one "pi-alkyl bond" constricts with TYR A:132 amino acid residues at a distance of 5.17 Å of distance (Figure 5).

Regarding the other mixture ingredient, "ciprofloxacin," an analysis of molecular docking for interaction with the Tankyrase enzyme revealed one "conventional hydrogen bond" formed with HIS A:120 amino acid residues at a distance of 2.83 Å, one "carbon-hydrogen bond" formed with HIS A:120 amino acid residues at a distance of 3.09 Å, two "pi-sigma bonds" formed with TYR A:1203 and TYR A:1224 amino acid residues at distances of 3.84 Å and 3.45 Å, one "pi-pi-stacked bond" formed with TYR A:1203 amino acid residues at a distance of 5.03 Å, one "alkyl bond" formed with two ILE A:1212 amino acid residues at a distance of 5.36 Å, and finally, one "pi-alkyl bound" formed with HIS A:1184 amino acid residues at a distance of 4.87 Å distance (Supplementary Figure 1).

For comparative purposes, a molecular docking study assessed the interaction between G007-LK (Tankyrase inhibitors) [59]. And the Tankyrase enzyme. This resulted in a docking score of (-9.2) kcal/mol for binding,

highlighting one "conventional hydrogen bond" formed with HIS A:1201 amino acid residues at a distance of 2.20 Å. Additionally, one "pi-pi-stacked bond" forms with TYR A:1224 amino acid residues at a distance of 3.73 Å. Lastly, one "pi-alkyl bond" interacts with ILE A:1204 amino acid residues at a distance of 5.31 Å (Supplementary Figure 2).

To clarify the effectiveness of the mixture's ability to target regulatory signals of the EMT pathway, a comparison of its docking score with standard medications that target the same regulatory signals of the EMT pathway was performed (Supplementary Table 4).

Drug Interaction Mapping (Combination Index- CI)

The CI score revealed a diverse combination pattern between the mixture ingredients. After 24 hours of incubation, concentrations of 0.1, 1, and 10 µg/ml showed very strong synergism, while 100 μg/ml exhibited strong synergism. Furthermore, 1000 μg/ml illustrated a pattern of synergistic effects.

After 72 hours of incubation, all concentrations showed a very strong synergistic effect pattern Supplementary Table (5,6) Supplementary Figure (3,4).

(dose reduction index- DRI)

During each incubation period and across all concentrations, the DRI score exceeded 1, indicating that the concentration of each ingredient in the mixture that led to significant cytotoxicity was lower than the significant cytotoxic concentrations of each ingredient when used separately. This reduction in concentrations suggests a lower likelihood of side effects from the mixture compared to the risks of side effects associated with each drug when used individually (Supplementary Tables (5,6) Supplementary Figures (3,4)).

Morphological Observations of HeLa Cancer Cells

Figure 10 shows the morphological changes in the HeLa and NHF cell lines after 72 hours of treatment.

Discussion

One option to explore an effective and safer alternative

anticancer drug is repositioning currently available non-anticancer medicines. In line with this concept, this study examined the anticancer effects of combining the antibacterial ciprofloxacin with the anticoagulant rivaroxaban. Drug selection is supported by multiple prior studies suggesting that both possess anticancer properties. Additionally, a comprehensive evaluation of the pharmacokinetics and safety of each medication was conducted.

The MTT cytotoxicity assay results showed that the mixture of rivaroxaban and ciprofloxacin inhibited cervical cancer proliferation while demonstrating lower cytotoxicity to normal cell lines. This combination displayed superior anticancer effectiveness compared to carboplatin and each mixture's individually medications.

The combination index score indicates that the two drugs work together synergistically. The dosage reduction index score also suggests that the combination carries a lower risk of adverse effects than individual drugs. The safety of the mixture is further supported by its favorable selectivity index score, which shows that it selectively targets cancer cells while sparing healthy ones.

The mixture's anticancer properties can be understood from two perspectives: first, by assessing the suggested anticancer mechanisms of each component from various previous studies, and second, by the novel anticancer mechanism proposed in the current molecular docking study.

Several studies assessed the anticancer effects of rivaroxaban. One study found that rivaroxaban could decrease cancer growth and invasion in mice with fibrosarcoma. A suggested mechanism is its role in boosting immune response against cancer, particularly by increasing the presence of dendritic and cytotoxic T-cells [61]. A different study reveals that Rivaroxaban enhances immunotherapy, leading to more significant cancer growth inhibition than immunotherapy alone. It activates CD103 + F4/80 - CCR7 + dendritic cells and GrB + cytotoxic CD8+ T cells specifically in the tumor microenvironment [62, 63]. Another study shows that rivaroxaban exerts an antiangiogenic effect in a dose-dependent manner, achieving a score of 0.7 at a concentration of 10-4 µmol/l [64]. Conversely, another study showed that although the direct oral anticoagulants rivaroxaban and dabigatran effectively suppress coagulation, they did not impede the growth and spread of cancer in orthotopic models [65].

Additionally, various studies have explored the anticancer properties of ciprofloxacin. A recent survey of repurposing this fluoroquinolone antibiotic revealed its potential as an anticancer agent. Ciprofloxacin is a drug used to treat bacterial infections. Researchers are interested in how it affects DNA gyrase and topoisomerase IV, which are enzymes in prokaryotes. This has led to studies on its impact on topoisomerases in eukaryotes, particularly because these enzymes are often overproduced in cancer cells to help them grow quickly. Another in vitro study has demonstrated that ciprofloxacin can trigger apoptosis and induce cell cycle arrest in multiple cancer cell lines. Research on colorectal cancer cells indicated that ciprofloxacin, in concentrations of 50–100 μM , activates caspase-3 and lowers levels of cyclin D1. This

process leads to a stop in the G1 phase of the cell cycle [66-69]. Likewise, in non-small cell lung cancer (A549 cells), ciprofloxacin reduced metastasis by dampening epithelial-mesenchymal transition (EMT) via modulation of the TGF-β/Smad3 pathway [70, 71].

Animal models verify these conclusions. A recent study utilizing xenograft mice with triple-negative breast cancer (MDA-MB-231 cells) showed that a daily administration of ciprofloxacin (20 mg/kg) resulted in a 40% reduction in tumor development, attributed to ROS-induced DNA damage and upregulation of p53 activation [72].

Alongside the previously discussed anticancer mechanisms for each mixture ingredient, the present study explores new anticancer mechanisms of rivaroxaban and ciprofloxacin, The molecular docking results indicate their potential to inhibit two necessary cancer enzymes: matrix metalloproteinase, targeted by rivaroxaban, and Tankyrase, targeted by ciprofloxacin, with respective docking scores of -9 kcal/mol and -8.9 kcal/mol.

Both of these enzymes are crucial for cancer. Matrix metalloproteinases (MMPs) are pivotal in cancer progression, as they degrade extracellular matrix (ECM) components, which aid tumor invasion, metastasis, and angiogenesis. These zinc-dependent endopeptidases are upregulated in various cancers, encouraging the breakdown of basement membranes and allowing cancer cells to infiltrate surrounding tissues and blood vessels. Notably, MMP-2 and MMP-9 are closely linked to tumor aggressiveness because of their capability to cleave type IV collagen, a key structural protein in the ECM. Furthermore, MMPs influence signalling in the tumor microenvironment by liberating growth factors and cytokines, thereby enhancing cancer cell proliferation and immune evasion. Recent research underscores the dual role of MMPs in cancer. Some isoforms demonstrate tumour-suppressive effects depending on the context and substrate specificity. For example, MMP-8 has been shown to inhibit melanoma progression by stimulating anti-tumor immune responses [73-75] .

Matrix metalloproteinases (MMPs), especially MMP-2 and MMP-9, significantly contribute to cervical cancer progression by breaking down extracellular matrix components, enhancing tumor invasion and metastasis. Their increased expression correlates with later stages of the disease and a poorer prognosis. Additionally, MMPs influence angiogenesis and immune evasion, which increases tumor aggressiveness. A recent study underscores the potential of MMPs as biomarkers and therapeutic targets in cervical cancer [76].

Several studies investigated MMP-targeted therapies, such as selective inhibitors and monoclonal antibodies, to mitigate their pro-tumorigenic properties while preserving normal physiological function functions [77]. However, clinical success is still limited due to the complexity of MMP interactions within the tumor microenvironment [78].

Additionally, Tankyrase (TNKS), an enzyme belonging to the poly (ADP-ribose) polymerase (PARP) family, is crucial in cancer progression as it regulates Wnt/ β -catenin signaling, maintains telomeres, and promotes cellular proliferation. Through its Parylation, Tankyrase stabilizes

AXIN2, a vital part of the β -catenin destruction complex, activating the Wnt pathway a characteristic of various cancers, including those of the colorectal, breast, and ovarian types. Elevated levels of Tankyrase correlate with increased cancer stemness, metastasis, and resistance to chemotherapy, positioning it as a valuable target for therapy. Moreover, recent research has suggested Tankyrase's role in altering the tumor microenvironment, affecting immune evasion and angiogenesis [28]. Due to their crucial role in cancer, small-molecule inhibitors like XAV939 and G007-LK selectively inhibit Tankyrase activity, suppressing Wnt-driven tumor growth in preclinical models [29]. Despite progress, clinical efficacy faces challenges from off-target effects and compensatory signalling pathways. New studies are investigating combination therapies that pair Tankyrase inhibitors with immune checkpoint blockers or traditional chemotherapeutics to boost anti-tumor responses [30].

The aforementioned role of each enzyme in cancer is primarily related to inhibiting cancer metastasis, particularly through the EMT pathway. According to the findings of our molecular docking study, the present study employed a combination of drugs, each demonstrating the ability to target Tankyrase and matrix metalloprotease enzymes. Tankyrase and matrix metalloproteinases drive epithelial-mesenchymal transition (EMT) and cancer metastasis. Tankyrase, by regulating the Wnt/β-catenin pathway, promotes EMT by downregulating E-cadherin and upregulating N-cadherin and vimentin, key markers of mesenchymal transition. Meanwhile, MMPs, particularly MMP-2 and MMP-9, facilitate ECM degradation, enabling tumor cell invasion and dissemination. Recent studies have revealed that TNKS enhances MMP expression through Wnt/β-catenin signalling, creating a feed-forward loop that amplifies metastatic potential [31-33]. In cervical and breast cancers, the TNKS-MMP pathway is associated with advanced tumor stages and reduced survival rates

Findings from our study's wound healing assay support the previously suggested mechanism by which the rivaroxaban-ciprofloxacin mixture inhibits cervical cancer metastasis. The mixture's ability to delay wound closure after 24 hours of incubation shows a superior impact compared to the effects of rivaroxaban and ciprofloxacin when used individually. This suggests a synergistic pattern in the combination of these medications, particularly at 24 hours of incubation. The combination index score further supports this.

Tankyrase and matrix metalloprotease enzymes play a crucial role in cancer, positioning them as promising targets for effective treatment therapies. Several trials were performed to identify Tankyrase inhibitors, such as (XAV939) [79], G007-LK [36], E7449 [37] and AZ6102[38]. Along these lines, several attempts were made to identify an agent that targets the matrix metalloprotease enzymes. Such as Marimastat [39], Tanomastat [40] and Ecaliximab [41]

Although several Tankyrase and matrix metalloprotease enzyme inhibitors have been identified, their use remains challenging. These include toxicity and side effects, the development of resistance, limited efficacy in specific cancers, a narrow therapeutic range, and high costs [42, 43, 80, 81]. These consequences motivate us to conduct this current study.

The study presents limitations, notably in laboratory validation related to the molecular analysis, attributed to various factors, including financial constraints.

In conclusion, this study aimed to identify an effective and safe anticancer option by repurposing a combination of two marketed medications (rivaroxaban and ciprofloxacin) for malignant cervical cancer treatment. MTT assay findings indicate that the mixture of rivaroxaban and ciprofloxacin significantly inhibits cervical cancer growth compared to the cytotoxicity of carboplatin, linagliptin, and rivaroxaban alone. Rivaroxaban and ciprofloxacin exhibit synergistic effects when used in combination, as indicated by the combination index score, particularly after 72 hours of treatment incubation. Regarding safety, the effective cytotoxic concentrations of the drugs in the mixture were lower than when used individually, indicating that the mixture is less likely to cause adverse effects. The mixture displays a favorable selectivity index, suggesting it selectively targets cancer cells rather than healthy cells. Moreover, the mixture demonstrated the ability to delay cancer metastasis, as shown by the wound healing assay results, indicating it reduces cancer cell migration by 98% and is significantly more effective than the individual effects of rivaroxaban and ciprofloxacin.

The study explores a novel anticancer mechanism of the mixture, demonstrating dual targeting of two crucial enzymes in the EMT pathway: matrix metalloproteinase enzyme targeting by rivaroxaban and Tankyrase targeting by ciprofloxacin, with molecular docking scores of -9 and -8.9 kcal/mol, respectively. This novel mechanism elucidates the anticancer and antimetastatic effects of the mixture. Furthermore, this mechanism clarifies the synesthetic effects of a complementary anticancer mechanism.

Based on these findings, the combination of rivaroxaban and ciprofloxacin presents a promising and safer alternative for treating cervical cancer, particularly considering their well-established pharmacokinetic and safety profiles.

Author Contribution Statement

Design and development, Gathering and organizing data, Data analysis/interpretation, Article composition, Critique the essay for significant ideas, Statistical analysis expertise, Ultimate article endorsement and guarantee: Alyaa Aziz Ahmed.

Acknowledgements

The research team thanks the researchers and instructional staff at ICMGR / al-Mustansiriyah University and the Iraqi National Cancer Research Center/University of Baghdad for their essential support throughout this study. I also wish to express my genuine appreciation to the quality control team at the Samarra Pharmaceutical Factory for providing the drugs utilized in this research.

Declaration of Generative AI and AI-assisted technologies in the writing process

The authors clarify that this work does not use generative AI or AI-assisted technologies.

Conflicts of interest

The authors state they have no conflicts of interest.

Abbreviations

(ICCMGR): The Iraqi Centre for Cancer and Medical Genetics Research.

MTT: 3-(4,5-dimethylthiazol-2-yl)-2,5-diphenyltetrazolium bromide stain

MEM: Minimum Essential Medium SAS: Statistical Analysis System

SD: Standard deviation

LSD: Least Significant Difference

DRI: dose reduction index CI: combination index WHA: wound healing assay

NHF cell line: human-derived adipose tissue cell line

EMT: epithelial-mesenchymal transition MMPs: matrix metalloprotease enzyme

TNKs: Tankyrase enzyme ECM: extracellular matrix

References

- Yuk JS, Lee B, Kim MH, Kim K, Seo YS, Hwang SO, et al. Incidence and risk factors of vte in patients with cervical cancer using the korean national health insurance data. Sci Rep. 2021;11(1):8031. https://doi.org/10.1038/s41598-021-87606-z
- 2. Arbyn M, Weiderpass E, Bruni L, de Sanjose S, Saraiya M, Ferlay J, et al. Estimates of incidence and mortality of cervical cancer in 2018: A worldwide analysis. Lancet Glob Health. 2020;8(2):e191-e203. https://doi.org/10.1016/S2214-109X(19)30482-6.
- 3. Khashman BM, Abdulla KN, Karim S, Alhashimi S, Mohammed ML, Sarah NA. The effect of twist expression on the development ofcervical carcinoma in a group of iraqi women infected with hpv. Biochem Cell Arch. 2019;19(2):3913-6.
- 4. Bruni L, Serrano B, Roura E, Alemany L, Cowan M, Herrero R, et al. Cervical cancer screening programmes and age-specific coverage estimates for 202 countries and territories worldwide: A review and synthetic analysis. Lancet Glob Health. 2022;10(8):e1115-e27. https://doi.org/10.1016/S2214-109X(22)00241-8.
- Abdulla KN, Aljebori S, Dh H, Mohson KI, Sabah Rasoul N, Mahdi MA. Risk factors for cervical cancer in iraqi women. Libri Oncologici: Croatian Journal of Oncology. 2023;51(2-3):59-64.
- Cohen PA, Jhingran A, Oaknin A, Denny L. Cervical cancer. Lancet. 2019;393(10167):169-82. https://doi.org/10.1016/ S0140-6736(18)32470-X.
- 7. Network CGAR. Integrated genomic and molecular characterization of cervical cancer. Nature. 2017;543(7645):378.
- 8. Hashim WS, Yasin YS, Jumaa AH, Al-Zuhairi MI, Abdulkareem AH. Physiological scrutiny to appraise a flavonol versus statins. Biomedical and Pharmacology Journal. 2023;16(1):289-93.
- 9. Abdulla KN, Abid SJ, Salih SR, Alheshimi SJ, Al-Attar Z.

- Most common risk factors distribution for cervical cancer. Revista Latinoamericana de Hipertension. 2024;19(3):128-32
- Cohen AC, Roane BM, Leath CA, 3rd. Novel therapeutics for recurrent cervical cancer: Moving towards personalized therapy. Drugs. 2020;80(3):217-27. https://doi.org/10.1007/ s40265-019-01249-z.
- 11. Khalifa MF, Ghadhban AGZA, Hade IM, Ali MM. Evaluation of quality of life for women with breast cancer. Scripta Medica. 2024;55(1):115-8.
- 12. Pfaendler KS, Tewari KS. Changing paradigms in the systemic treatment of advanced cervical cancer. Am J Obstet Gynecol. 2016;214(1):22-30. https://doi.org/10.1016/j.ajog.2015.07.022.
- 13. Jumaa AH, Al Uboody WSH, Hady AM. Esomeprazole and amygdalin combination cytotoxic effect on human cervical cancer cell line (hela cancer cell line). Int J Pharm Sci Res. 2018;10(9):2236-41.
- Jumaa AH, Jarad AS, Al Uboody WSH. The effect of esomeprazole on cell line human cervical cancer. Medico-Legal Update. 2020;20(1).
- 15. Jumaa AH, Abdulkareem AH, Yasin YS. The cytotoxic effect of ciprofloxacin laetrile combination on esophageal cancer cell line. Asian Pac J Cancer Prev. 2024;25(4):1433-40. https://doi.org/10.31557/APJCP.2024.25.4.1433.
- Said AM, Abdulla KN, Ahmed NH, Yasin YS. Antiproliferative impact of linagliptin on the cervical cancer cell line. Asian Pac J Cancer Prev. 2024;25(9):3293. https://doi. org/10.31557/APJCP.2024.25.9.3293
- 17. Ahmed A, Nihad A, Sabreen G, Youssef Y, Azal J. Synergistic antiproliferative effect of linagliptin-metformin combination on the growth of hela cancer cell line. Journal of Cancer Research Updates. 2025;14:12-23. https://doi.org/10.30683/1929-2279.2025.14.02.
- 18. Arean AG, Jumaa AH, Hashim WS, Mohamed AA, Yasin YS. The cytotoxic effect of ephedra transitoria on hela cancer cell line: Bio-engineering.
- Yasin Al-Samarray YS, Jumaa AH, Hashim WS, Khudhair YI.
 The cytotoxic effect of ethanolic extract of cnicus benedictus
 1. Flowers on the murine mammary adenocarcinoma cancer cell line amn-3. Biochemical & Cellular Archives. 2020;20.
- Abdulla KN, Khudhur RK, Said AM, Jumaa AH, Yasin YS. Laetrile and methotrexate: A dual-drug approach to inhibiting cervical cancer cell proliferation. J Cancer Res Updates. 2025;14:52-62. https://doi.org/10.30683/1929-2279.2025.14.06.
- Khudhur RK, Yahiya YI, Majeed AH, Yasin YS, Jumaa AH. Scrutiny of the co-cytotoxic impact of metformin-omeprazole on the cervical cancer cell line and their aptitude to target heat shock 60. Asian Pac J Cancer Prev. 2025;26(4):1353-63. https://doi.org/10.31557/APJCP.2025.26.4.1353.
- 22. Maqsood A, Hisada Y, Garratt KB, Homeister J, Mackman N. Rivaroxaban does not affect growth of human pancreatic tumors in mice. J Thromb Haemost. 2019;17(12):2169-73. https://doi.org/10.1111/jth.14604.
- Noble S. Venous thromboembolism and palliative care. Clin Med (Lond). 2019;19(4):315-8. https://doi.org/10.7861/ clinmedicine.19-4-315.
- 24. Zhou S, Xiao Y, Zhou C, Zheng Z, Jiang W, Shen Q, et al. Effect of rivaroxaban vs enoxaparin on major cardiac adverse events and bleeding risk in the acute phase of acute coronary syndrome: The h-replace randomized equivalence and noninferiority trial. JAMA Netw Open. 2023;6(2):e2255709. https://doi.org/10.1001/jamanetworkopen.2022.55709.
- 25. Zhou H, Chen TT, Ye LL, Ma JJ, Zhang JH. Efficacy and safety of direct oral anticoagulants versus low-molecularweight heparin for thromboprophylaxis after cancer surgery:

- A systematic review and meta-analysis. World J Surg Oncol. 2024;22(1):69. https://doi.org/10.1186/s12957-024-03341-5
- Recber T, Haznedaroglu IC, Celebier M. Review on characteristics and analytical methods of rivaroxaban. Crit Rev Anal Chem. 2022;52(4):865-77. https://doi.org/10.108 0/10408347.2020.1839735.
- 27. Saboowala HK. What hela cells aka immortal cells are and why they are important. An example of racism in medicine. Dr. Hakim Saboowala; 2022.
- Kim MK. Novel insight into the function of tankyrase. Oncol Lett. 2018;16(6):6895-902. https://doi.org/10.3892/ ol.2018.9551.
- Kamal A, Riyaz S, Srivastava AK, Rahim A. Tankyrase inhibitors as therapeutic targets for cancer. Curr Top Med Chem. 2014;14(17):1967-76. https://doi.org/10.2174/1568 026614666140929115831.
- Verma A, Kumar A, Chugh A, Kumar S, Kumar P. Tankyrase inhibitors: Emerging and promising therapeutics for cancer treatment. Med Chem Res. 2021;30:50-73. https://doi. org/10.1007/s00044-020-02657-7
- 31. Huang J, Qu Q, Guo Y, Xiang Y, Feng D. Tankyrases/beta-catenin signaling pathway as an anti-proliferation and anti-metastatic target in hepatocarcinoma cell lines. J Cancer. 2020;11(2):432-40. https://doi.org/10.7150/jca.30976.
- 32. Piperigkou Z, Kyriakopoulou K, Koutsakis C, Mastronikolis S, Karamanos NK. Key matrix remodeling enzymes: Functions and targeting in cancer. Cancers (Basel). 2021;13(6):1441. https://doi.org/10.3390/cancers13061441.
- 33. Du F, Li J, Zhong X, Zhang Z, Zhao Y. Endothelial-to-mesenchymal transition in the tumor microenvironment: Roles of transforming growth factor-beta and matrix metalloproteins. Heliyon. 2024;10(21):e40118. https://doi.org/10.1016/j.heliyon.2024.e40118.
- 34. Song P, Gao Z, Bao Y, Chen L, Huang Y, Liu Y, et al. Wnt/beta-catenin signaling pathway in carcinogenesis and cancer therapy. J Hematol Oncol. 2024;17(1):46. https://doi.org/10.1186/s13045-024-01563-4.
- 35. Ibrahim NM, Fahim SH, Hassan M, Farag AE, Georgey HH. Design and synthesis of ciprofloxacin-sulfonamide hybrids to manipulate ciprofloxacin pharmacological qualities: Potency and side effects. Eur J Med Chem. 2022;228:114021. https://doi.org/10.1016/j.ejmech.2021.114021
- 36. Shiraishi A, Oh-Hara T, Takahashi Y, Uchibori K, Nishio M, Katayama R. 3d layered co-culture model enhances trastuzumab deruxtecan sensitivity and reveals the combined effect with g007-lk in her2-positive non-small cell lung cancer. Biochem Biophys Res Commun. 2024;725:150255. https://doi.org/10.1016/j.bbrc.2024.150255.
- Plummer R, Dua D, Cresti N, Drew Y, Stephens P, Foegh M, et al. First-in-human study of the parp/tankyrase inhibitor e7449 in patients with advanced solid tumours and evaluation of a novel drug-response predictor. Br J Cancer. 2020;123(4):525-33. https://doi.org/10.1038/s41416-020-0916-5
- 38. Yoshiura S, Fujimura T, Furugaki K, Mizuta H, Nishio M, Uchibori K, et al. Targeting ErbB and tankyrase1/2 prevent the emergence of drug tolerant persister cells in ALK fusion positive lung cancer; 2032.
- 39. Layfield HJ, Williams HF, Ravishankar D, Mehmi A, Sonavane M, Salim A, et al. Repurposing cancer drugs batimastat and marimastat to inhibit the activity of a group i metalloprotease from the venom of the western diamondback rattlesnake, crotalus atrox. Toxins (Basel). 2020;12(5):309. https://doi.org/10.3390/toxins12050309.
- 40. Lim TYM, Jaladanki CK, Wong YH, Yogarajah T, Fan H, Chu JJH. Tanomastat exerts multi-targeted inhibitory effects

- on viral capsid dissociation and rna replication in human enteroviruses. EBioMedicine. 2024;107:105277. https://doi.org/10.1016/j.ebiom.2024.105277.
- 41. Shah MA, Cunningham D, Metges JP, Van Cutsem E, Wainberg Z, Elboudwarej E, et al. Randomized, open-label, phase 2 study of andecaliximab plus nivolumab versus nivolumab alone in advanced gastric cancer identifies biomarkers associated with survival. J Immunother Cancer. 2021;9(12):e003580. https://doi.org/10.1136/jitc-2021-003580.
- 42. Hong DS, Fakih MG, Strickler JH, Desai J, Durm GA, Shapiro GI, et al. Kras(g12c) inhibition with sotorasib in advanced solid tumors. N Engl J Med. 2020;383(13):1207-17. https://doi.org/10.1056/NEJMoa1917239.
- Canon J, Rex K, Saiki AY, Mohr C, Cooke K, Bagal D, et al. The clinical kras(g12c) inhibitor amg 510 drives antitumour immunity. Nature. 2019;575(7781):217-23. https:// doi.org/10.1038/s41586-019-1694-1.
- Lyapun I, Andryukov B, Bynina M. Hela cell culture: Immortal heritage of henrietta lacks. Mol Genet Microbiol Virol. 2019;34(4):195-200. https://doi.org/10.3103/ S0891416819040050.
- 45. Safi IN, Mohammed Ali Hussein B, Al-Shammari AM. In vitro periodontal ligament cell expansion by co-culture method and formation of multi-layered periodontal ligamentderived cell sheets. Regen Ther. 2019;11:225-39. https://doi. org/10.1016/j.reth.2019.08.002.
- Souren NY, Fusenig NE, Heck S, Dirks WG, Capes-Davis A, Bianchini F, et al. Cell line authentication: A necessity for reproducible biomedical research. EMBO J. 2022;41(14):e111307. https://doi.org/10.15252/embj.2022111307.
- 47. Le Berre M, Gerlach JQ, Dziembala I, Kilcoyne M. Calculating half maximal inhibitory concentration (ic(50)) values from glycomics microarray data using graphpad prism. Methods Mol Biol. 2022;2460:89-111. https://doi.org/10.1007/978-1-0716-2148-6 6.
- 48. He Y, Zhu Q, Chen M, Huang Q, Wang W, Li Q, et al. The changing 50% inhibitory concentration (ic50) of cisplatin: A pilot study on the artifacts of the mtt assay and the precise measurement of density-dependent chemoresistance in ovarian cancer. Oncotarget. 2016;7(43):70803-21. https://doi.org/10.18632/oncotarget.12223.
- 49. Bezerra JN, Gomez MCV, Rolón M, Coronel C, Almeida-Bezerra JW, Fidelis KR, et al. Chemical composition, evaluation of antiparasitary and cytotoxic activity of the essential oil of psidium brownianum mart ex. Dc. Biocatal Agric Biotechnol. 2022;39:102247. https://doi.org/10.1016/j.bcab.2021.102247.
- Martinotti S, Ranzato E. Scratch wound healing assay. Methods Mol Biol. 2020;2109:225-9. https://doi. org/10.1007/7651 2019 259.
- Salentin S, Schreiber S, Haupt VJ, Adasme MF, Schroeder M. Plip: Fully automated protein-ligand interaction profiler. Nucleic Acids Res. 2015;43(W1):W443-7. https://doi. org/10.1093/nar/gkv315.
- Chen G, Seukep AJ, Guo M. Recent advances in molecular docking for the research and discovery of potential marine drugs. Mar Drugs. 2020;18(11):545. https://doi.org/10.3390/ md18110545.
- 53. Meyer CT, Wooten DJ, Lopez CF, Quaranta V. Charting the fragmented landscape of drug synergy. Trends Pharmacol Sci. 2020;41(4):266-80. https://doi.org/10.1016/j.tips.2020.01.011.
- 54. Chou T-CJS. The combination index (ci<1) as the definition of synergism and of synergy claims. Elsevier; 2018. p. 49-50. https://doi.org/10.1016/j.synres.2018.04.001

- 55. Cary NJSIIU. Statistical analysis system, user's guide. Statistical. Version 9. 2012.
- 56. da Fonseca ASA, de Souza Monteiro I, Dos Santos CR, Carneiro MLB, Morais SS, Araújo PL, et al. Effects of andiroba oil (carapa guianensis aublet) on the immune system in inflammation and wound healing: A scoping review. J Ethnopharmacol. 2024;327:118004. https://doi. org/10.1016/j.jep.2024.118004.
- 57. Guo L-Y, Xing X, Tong J-B, Li P, Ren L, An C-X. Qsar aided design of potent ret inhibitors using molecular docking, molecular dynamics simulation and binding free energy calculation. Molecular Dynamics Simulation and Binding Free Energy Calculation. 2024. https://doi.org/10.2139/ ssrn.4886845
- 58. Vergote I, Heitz F, Buderath P, Powell M, Sehouli J, Lee CM, et al. A randomized, double-blind, placebo-controlled phase 1b/2 study of ralimetinib, a p38 mapk inhibitor, plus gemcitabine and carboplatin versus gemcitabine and carboplatin for women with recurrent platinum-sensitive ovarian cancer. Gynecol Oncol. 2020;156(1):23-31. https://doi.org/10.1016/j.ygyno.2019.11.006.
- 59. Blair HA. Sotorasib: First approval. Drugs. 2021;81(13):1573-9. https://doi.org/10.1007/s40265-021-01574-2
- Mahdi HM, Wadee SA. Interaction effect of methotrexate and aspirin on mcf7 cell line proliferation: In vitro study. J Adv Vet Res. 2023;13(9):1767-71.
- 61. Graf C, Wilgenbus P, Pagel S, Pott J, Marini F, Reyda S, et al. Myeloid cell-synthesized coagulation factor x dampens antitumor immunity. Sci Immunol. 2019;4(39):eaaw8405. https://doi.org/10.1126/sciimmunol.aaw8405.
- 62. Salmi S, Halinen K, Lin A, Suikkanen S, Jokelainen O, Rahunen E, et al. The association of cd8+ cytotoxic t cells and granzyme b+ lymphocytes with immunosuppressive factors, tumor stage and prognosis in cutaneous melanoma. Biomedicines. 2022;10(12):3209. https://doi.org/10.3390/biomedicines10123209.
- 63. Roberts EW, Broz ML, Binnewies M, Headley MB, Nelson AE, Wolf DM, et al. Critical role for cd103(+)/cd141(+) dendritic cells bearing ccr7 for tumor antigen trafficking and priming of t cell immunity in melanoma. Cancer Cell. 2016;30(2):324-36. https://doi.org/10.1016/j.ccell.2016.06.003.
- 64. Yavuz C, Caliskan A, Karahan O, Yazici S, Guclu O, Demirtas S, et al. Investigation of the antiangiogenic behaviors of rivaroxaban and low molecular weight heparins. Blood Coagul Fibrinolysis. 2014;25(4):303-8. https://doi.org/10.1097/MBC.000000000000019.
- 65. Buijs JT, Laghmani EH, van den Akker RFP, Tieken C, Vletter EM, van der Molen KM, et al. The direct oral anticoagulants rivaroxaban and dabigatran do not inhibit orthotopic growth and metastasis of human breast cancer in mice. J Thromb Haemost. 2019;17(6):951-63. https://doi. org/10.1111/jth.14443.
- 66. Alaaeldin R, Nazmy MH, Abdel-Aziz M, Abuo-Rahma GEA, Fathy M. Cell cycle arrest and apoptotic effect of 7-(4-(n-substituted carbamoylmethyl) piperazin-1-yl) ciprofloxacin-derivative on hct 116 and a549 cancer cells. Anticancer Res. 2020;40(5):2739-49. https://doi.org/10.21873/anticanres.14245.
- 67. Ali DME, Aziz HA, Bräse S, Al Bahir A, Alkhammash A, Abuo-Rahma GE-DA, et al. Unveiling the anticancer potential of a new ciprofloxacin-chalcone hybrid as an inhibitor of topoisomerases i & ii and apoptotic inducer. Molecules. 2024;29(22):5382. https://doi.org/10.3390/molecules29225382
- 68. Pashapour N, Dehghan-Nayeri MJ, Babaei E, Khalaj-Kondori M, Mahdavi M. The assessment of cytotoxicity,

- apoptosis inducing activity and molecular docking of a new ciprofloxacin derivative in human leukemic cells. J Fluoresc. 2024;34(3):1379-89. https://doi.org/10.1007/s10895-023-03350-9
- 69. Jarad A, Hamoody A, Hasan M, Shwaish M, Farhan W, Ibrahim Z, et al. Diabetic wound healing enhancement by tadalafil. Int J Pharm Res. 2020;12:841-7. https://doi.org/10.31838/ijpr/2020.12.03.121
- 70. Fawzy MA, Abu-Baih RH, Abuo-Rahma GEA, Abdel-Rahman IM, El-Sheikh AAK, Nazmy MH. In vitro anticancer activity of novel ciprofloxacin mannich base in lung adenocarcinoma and high-grade serous ovarian cancer cell lines via attenuating mapk signaling pathway. Molecules. 2023;28(3):1137. https://doi.org/10.3390/molecules28031137.
- 71. Huang CY, Yang JL, Chen JJ, Tai SB, Yeh YH, Liu PF, et al. Fluoroquinolones suppress tgf-beta and pma-induced mmp-9 production in cancer cells: Implications in repurposing quinolone antibiotics for cancer treatment. Int J Mol Sci. 2021;22(21):11602. https://doi.org/10.3390/ijms222111602.
- Aravindan A, Gupta A, Moorkoth S, Dhas N. Implications of nanotherapeutic advancements to leverage multi-drug resistant breast cancer: The state-of-the-art review. J Drug Deliv Sci Technol. 2024:106007. https://doi.org/10.1016/j. jddst.2024.106007.
- Niland S, Riscanevo AX, Eble JA. Matrix metalloproteinases shape the tumor microenvironment in cancer progression. Int J Mol Sci. 2021;23(1):146. https://doi.org/10.3390/ ijms23010146.
- Mustafa S, Koran S, AlOmair L. Insights into the role of matrix metalloproteinases in cancer and its various therapeutic aspects: A review. Front Mol Biosci. 2022;9:896099. https://doi.org/10.3389/fmolb.2022.896099.
- 75. Cox TR. The matrix in cancer. Nat Rev Cancer. 2021;21(4):217-38. https://doi.org/10.1038/s41568-020-00329-7.
- 76. Chen W, Huang S, Shi K, Yi L, Liu Y, Liu W. Prognostic role of matrix metalloproteinases in cervical cancer: A meta-analysis. Cancer Control. 2021;28:10732748211033743. https://doi.org/10.1177/10732748211033743.
- 77. Bandopadhyay S, Dey U, Chakraborty P, Debnath P, Kundu S, Laik D, et al. The role of matrix metalloproteinases mmp2 and mmp9 in ovarian cancer progression. Handbook of proteases in cancer. CRC Press; 2025. p. 100-12.
- 78. Almutairi S, Kalloush HM, Manoon NA, Bardaweel SK. Matrix metalloproteinases inhibitors in cancer treatment: An updated review (2013-2023). Molecules. 2023;28(14):5567. https://doi.org/10.3390/molecules28145567.
- Pundkar C, Antony F, Kang X, Mishra A, Babu RJ, Chen P, et al. Targeting wnt/beta-catenin signaling using xav939 nanoparticles in tumor microenvironmentconditioned macrophages promote immunogenicity. Heliyon. 2023;9(6):e16688. https://doi.org/10.1016/j. heliyon.2023.e16688
- 80. Dienstmann R, Salazar R, Tabernero J. Overcoming resistance to anti-egfr therapy in colorectal cancer. Am Soc Clin Oncol Educ Book. 2015;35(1):e149-56. https://doi.org/10.14694/EdBook AM.2015.35.e149.
- 81. Cheng Y, Tian H. Current development status of mek inhibitors. Molecules. 2017;22(10):1551. https://doi.org/10.3390/molecules22101551.



This work is licensed under a Creative Commons Attribution-Non Commercial 4.0 International License.